Development of Self-Healing Multifunctional Materials

Liberata Guadagno[1*], Carlo Naddeo[1], Marialuigia Raimondo[1], Giuseppina Barra[1], Luigi Vertuccio[1*], Andrea Sorrentino[2], Wolfgang Binder[3], Martin Kadlec[4]

[1]Department of Industrial Engineering, University of Salerno, Via Giovanni Paolo II, 132 - 84084 Fisciano (SA), Italy

[2]Institute for Polymers, Composites and Biomaterials (IPCB), National Research Council (CNR), Via Previati 1/C, 23900 Lecco, Italy

[3] Macromolecular Chemistry, Institute of Chemistry, Division of Technical and Macromolecular Chemistry, Faculty of Natural Science II (Chemistry, Physics and Mathematics), Martin-Luther-University Halle-Wittenberg, Danckelmann-Platz 4, Halle, Germany

[4]VZLU – Aerospace Research and Test Establishment, Beranovych 130, Prague, Czech Republic

***Corresponding author**

Liberata Guadagno - e-mail: lguadagno@unisa.it

phone +39 089964114

mobile +39 3204213235

Luigi Vertuccio – e-mail: lvertuccio@unisa.it

ABSTRACT

Reversible hydrogen bonds determined by interaction between epoxy resin and nanocages of polyhedral oligomeric silsesquioxane (POSS) compound have been employed to activate self-healing mechanisms integrated in thermosetting multifunctional materials. The phase composition of the multifunctional resin containing embedded multiwalled carbon nanotubes (MWCNT) can be advantageously exploited to enhance the healing efficiency up to 400%. The presence of MWCNT is responsible of a greater mobility of chains belonging to domains finely interpenetrated in the matrix where the reversible hydrogen bonds can provide enhanced healing efficiency.

Keywords: A. Nano-structures; A. Thermosetting resins; A. Smart materials; A. Polymer-matrix composites (PMCs)

1. Introduction

The investigation of strategies to impart auto-repair functions to polymeric materials is an emerging and fascinating area of research. They promise to significantly extend the working life and safety of the structural components for a broad range of applications (such as aeronautics, shipbuilding industries, wind turbine blades, active implantable medical devices etc.). Several self-healing concepts for polymeric materials have been published over the last 15 years. Depending on the chemical nature of the polymer matrix, different approaches have been proposed to prepare self-healing systems. However, the hardest challenge in this field is to develop a structural self-healing material capable of repairing itself in its working environment and does it quickly without any external intervention. In the case of materials characterized by relatively low glass transition temperature, the movement of the macromolecular chains (or segment of chains) makes possible the use of different self-healing mechanisms. On the opposite, for "structural material" characterized by high stiffness or limited movement of the molecular chains, only limited choices in the self-healing mechanisms can really allow successful results. In fact, the development of smart composites capable of self-repair in load-bearing structures is still at the planning stage owing to complex issues to overcome. For structural materials, one of the most promising extrinsic self-healing approaches (based on epoxy resins-Epon 828) was proposed by White et al. [1]. This system consists of incorporating a microencapsulated healing agent and a catalytic chemical trigger within an epoxy matrix. An approaching crack ruptures embedded microcapsules and allows releasing of a polymerizer agent into the crack plane through capillary action. Ring-Opening Metathesis Polymerization (ROMP) of the healing agent is triggered by contact with the embedded catalyst, bonding the crack faces. After the milestone work reported by White and co-workers, self-healing chemistry for thermosetting polymers was rapidly expanded in the past decade. A great number of self-healing thermosetting systems based on extrinsic or intrinsic mechanisms have been demonstrated. Crosslinking methods relying on epoxy [2], "click-chemistry" based [3] and thiol/ene-based systems [4] have been developed. However, the ROMP-based healing agents remain the main design proposed for the develop of structural self-healing materials [5-12]. Among the others, those based on first-generation Grubbs' catalyst (G1) [13-17], second-generation Grubbs' catalyst (G2) and Hoveyda-Grubbs' second-generation catalyst (HG2) are currently under evaluation [18]. These systems promise to be a solution for epoxy structural composites where no soft matter or thermoplastic matrix is present. However, some drawbacks must be overcome in order to obtain materials for advanced applications. One of these concerns the thermal stability of the ruthenium catalysts inside the epoxy resin during the curing cycle [18-19]. In fact, high temperatures of the curing cycles planned for high

performances epoxy formulations can leave to a thermolytic decomposition of the ruthenium catalysts [18-24]. More in general, poor mechanical performance of the actual self-healing materials is due to different factors: a) the impossibility to use hardeners as aromatic primary amines (e.g. 4,4'-diaminodiphenylsulfone - DDS) in combination with catalysts active in the ROMP; b) the impossibility to use curing cycles at high temperatures; c) the impossibility to use the catalyst dispersed in the form of molecular complex in chemically very reactive environments, such as fluid epoxy mixtures containing reactive epoxy rings at high temperatures [21]. In fact, the maximum glass transition temperature (Tg) reached was between 100°C and 115°C, whereas the value of the storage modulus (between -50°C and + 80°C) was found to ranging between 2500 MPa and 2000 MPa. In order to increase the mechanical performance and simultaneously improve other functionalities such as electrical conductivity, different nanofillers were embedded in the epoxy matrix [25-36]. In particular, the work reported in ref. [27] showed that graphene-based nanomaterials can be designed as a self-assembly structure in the epoxy matrices using edge-carboxylated layers approach. Grubbs catalysts 1st (G1) and 2nd generation modified (G2o-tol), Hoveyda-Grubbs catalysts 1st (HG1) and 2nd generation (HG2) were covalently bonded to GO (graphene oxide) preserving the same catalytic activity of the catalysts not bonded to the graphene sheets. GO-G2 o-tol and GO-G1 were found to deactivate during the process of preparation of the self-healing epoxy mixtures at 90°C [25]. The self-healing activity of the various catalytic complexes was studied for both uncured and cured samples. Results showed that GO-HG1 and GO-HG2 were not deactivated and hence they were found to be able to trigger self-healing reactions based on the ROMP of 5-ethylidene-2-norbornene (ENB). This behavior was found due to the formation of 16 electron Ru-complexes that are more stable than the 14 electron complexes of GO-G1 and GO-G2 catalysts [25]. A strong increase in the storage modulus was found (as expected), but no in the glass transition temperature. In this case, it was also found that aromatic amines, necessary to obtain epoxy matrix with very high performance, could not be used as hardener [25].

Unfortunately, many of the structural applications require that the function of self-healing must be activated under extreme environmental conditions and the self-healing mechanisms must be quickly activated to avoid the crack propagation (when the entity of the propagation is relevant there is no healing of the material). Furthermore, the materials for many very interesting structural applications must be characterized by very high mechanical performances, electrical and thermal conductivity, low moisture content, long durability etc. Recent developments on self-healing system based on microencapsulation strategy have also demonstrated that these kinds of materials are also characterized by an improved ability to dissipate vibration energy and by a higher damping coefficient compared to standard Carbon Fiber Reinforced

Composites (CFRC) [37]. The critical points of these systems are very relevant when carbon fiber reinforced composites are impregnated with self-healing formulations based on these self-healing systems, due to infiltration problems and the distribution of the vessels and catalyst particles between the plies. Furthermore, these problems become even of bigger relevance when more complex hybrid architecture consisting of interleaved composite laminate are considered [38]. The above theoretical considerations have been the linchpin to develop new self-healing systems based on the presence of hydrogen bonding moieties on components of the epoxy formulation [39-40]. In particular, in the development of the self-healing formulations, the relevant need to impart self-healing functionality to multifunctional epoxy formulations at high mechanical performance must been considered. In this study, self-healing mechanisms in multifunctional thermosetting resins as an alternative to the microencapsulation concept and based on the possibility to activate reversible hydrogen bonding forces have been considered. The design of self-healing polymers based on hydrogen bonding combines highly dynamic properties, such as bonds showing a reversible "sticker-like" behavior enabling connection and reconnection, and thus supramolecular network formation. The challenge faced in the application of this approach was the limited dynamic properties of thermosetting matrix segments. The performed work highlighted that hydrogen bonding forces can be activated between oxygen belonging to specific nanocages of POSS compounds and O-H groups of epoxy network. These attractive interactions are favored by a suitable phase composition of the carbon nanoparticles containing formulation.

Furthermore, recent developments on the processing of these systems and in particular of those containing multiwalled carbon nanotubes have demonstrated that filtration problems, due to their attitude to form bundles because of their geometry and van der Walls forces, can be easily overcome using opportune dispersion techniques and modified infusion processes [41-43]. In this paper, acting on the phase composition and synergic effects between the added functionalities, multifunctional materials characterized by autorepair ability have been developed.

2. Experimental and Methods

2.1. Materials

2.1.1. Nanofilled resin

The epoxy matrix was prepared by mixing an epoxy precursor, tetraglycidylmethylenedianiline (TGMDA) (epoxy equivalent weight 117-133 g/eq), with an epoxy reactive monomer 1-4 butanedioldiglycidyl ether (BDE) that acts as a reactive diluent. The curing agent investigated for this study is 4,4-diaminodiphenyl

sulfone (DDS). The epoxy mixture was obtained by mixing TGMDA with BDE monomer at a concentration of 80%: 20% (by wt) epoxide to flexibilizer. Four different POSS compounds were dispersed in the epoxy matrix: Glycidyl POSS (GPOSS), TriglycidylCyclohexyl (TCPOSS) and Epoxycyclohexyl POSS (ECPOSS) functionalized with a different number of oxirane rings, and DodecaPhenyl POSS (DPHPOSS) functionalized with phenyl groups.

The curing agent DDS was added at a stoichiometric concentration with respect to all the epoxy rings (TGMDA, BDE and POSS - in the case of POSS with epoxy rings). The MWCNT (3100 Grade) were obtained from Nanocyl S.A. Transmission electron microscopy (TEM) investigation has shown for MWCNT an outer diameter ranging from 10 to 30 nm. The length of MWCNT is from hundreds of nanometers to some micrometer. The number of walls varies from 4 to 20 in most nanotubes. The specific surface area of MWCNT determined with the BET method is around 250-300 m^2/g; the carbon purity is > 95% with a metal oxide impurity of 5% as it results by thermogravimetric analysis. Epoxy blend and DDS were mixed at 120°C and the MWCNT were added and incorporated into the matrix by using an ultrasonication for 20 min. An ultrasonic device, Hielscher model UP200S (200 W, 24 kHz) was used. The epoxy mixture used to manufacture the panels was filled with 0.5 wt% of MWCNT. This nanofilled sample will be named hereunder T20BD+0.5% MWCNT. This concentration was chosen because the curves of DC volume conductivity vs MWCNT concentration highlight that the electrical percolation threshold (EPT) is lower than 0.32 wt%, therefore for this amount of MWCNT the nanofilled formulation is beyond the EPT [40]. This formulation is also characterized by good dynamic mechanical properties [44]. TGMDA, BDE, DDS were obtained from Sigma-Aldrich, and POSS compounds from Hybrid Plastics Company.

Epoxy blends and DDS were mixed at 120°C and all the samples were cured by a two-stage curing cycles: a first isothermal stage was carried out at the lower temperature of 125°C for 1 h and the second isothermal stage at higher temperatures up to 200°C for 3 h.

2.2. Methods

2.2.1. Dynamic mechanical analysis

Dynamic mechanical properties of the samples were performed with a dynamic mechanical thermo-analyzer (Tritec 2000 DMA -Triton Technology). Solid samples with dimensions 2 x 10 x 35 mm^3 were tested by applying a variable flexural deformation in three points bending mode. The displacement amplitude was set to 0.03 mm, whereas the measurements were performed at the frequency of 1 Hz. The range of temperature was from -90°C to 315°C at the scanning rate of 3°C/min.

2.2.2. SEM Analysis

Micrographs of the epoxy nanocomposites were obtained using Scanning Electron Microscope-SEM (mod. LEO 1525, Carl Zeiss SMT AG, Oberkochen, Germany). All samples were placed on a carbon tab previously stuck to an aluminum stub (Agar Scientific, Stansted, UK) and were covered with a 250 Å-thick gold film using a sputter coater (Agar mod. 108 A). Nanofilled sample sections were cut from solid samples by a sledge microtome. These slices were etched before the observation by SEM. The etching reagent was prepared by stirring 1.0 g potassium permanganate in a solution mixture of 95 mL sulfuric acid (95–97%) and 48 mL orthophosphoric acid (85%). The filled resins were immersed into the fresh etching reagent at room temperature and held under agitation for 36 h. Subsequent washings were done using a cold mixture of two parts by volume of concentrated sulfuric acid and seven parts of water. Afterward the samples were washed again with 30% aqueous hydrogen peroxide to remove any manganese dioxide. The samples were finally washed with distilled water and kept under vacuum for 5 days before being subjected to morphological analysis.

2.2.3. Self-Healing Efficiency Evaluation

To assess the crack-healing efficiency of the composite materials experiments were performed by using a dynamic mechanical thermo-analyzer (TA instrument-DMA 2980). Solid samples with dimensions 3 x 10 x 35 mm^3 were tested by applying a variable flexural deformation in single cantilever mode. A V-shaped starter notch, 1mm deep and 2 mm wide, was machined close to the sample extremity as shown in Fig. 1.

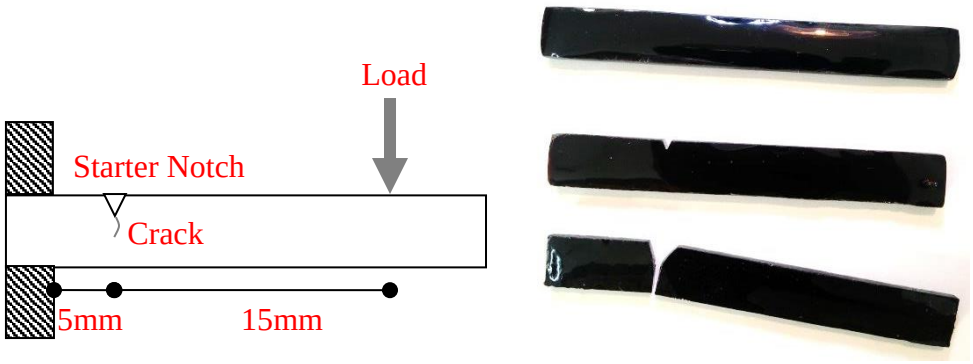

Fig. 1. Test geometry adapted for the healing tests (see on the left); epoxy specimens before and after healing experiments (see on the right).

The test procedure combines three different steps. In the first step, the notched sample was analysed under the dynamic flexural deformations for about 300 s in order to determine the pristine elastic modulus. After that, the oscillation was stopped and a sharp pre-crack was created in the samples by gently tapping a fresh

razor blade into a machined starter notch. An impulsive load of about 25 N was immediately applied to the specimen in order to produce crack propagation along the virgin crack plane. At this point, the dynamic monitoring of the sample was conducted at constant temperature, with a displacement amplitude set to 0.1% and a frequency to 1 Hz. Several test conditions were investigated in order to obtain a reasonable picture of the amount and time of recovery without influencing the healing mechanisms. The infrared spectra were obtained at 200°C (after the curing cycle) by using a Bruker Vertex 70 FTIR spectrophotometer with a 2 cm^{-1} resolution (64 scans collected).

2.2.4. Rheological measurements

Rheologial measurements were performed using a Rheometer AR 2000 TA Instruments. Parallel plates (ϕ = 40 mm) were selected as appropriate geometry and the gap was set at a value of 300 μm. Temperature sweeps from 80 to 180°C were carried out at constant frequency of 1 Hz at strain% set at 5% within the linear viscoelastic region (determined by strain sweep test).

3. Results and discussion

3.1. Dynamic Mechanical Analysis (DMA)

In order to understand the effect of MWCNT on the mechanical properties, DMA was performed for the analysed samples. The storage modulus, E' (MPa), and the loss factor, tanδ, are shown in Figs. 2 and 3 respectively.

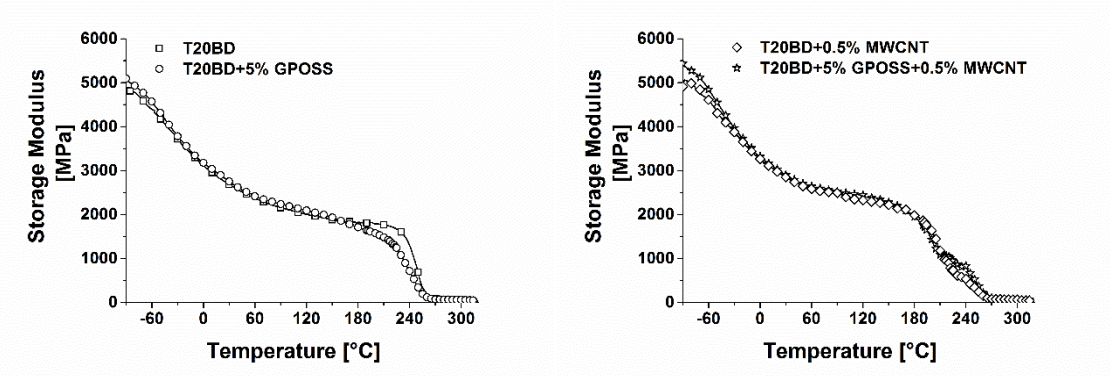

Fig. 2. Storage modulus of the unfilled epoxy formulations T20BD, T20BD+5%GPOSS (see on the left); Storage modulus of the epoxy formulations loaded with 0.5% by wt of MWCNT: T20BD+0.5% MWCNT, T20BD+5%GPOSS+0.5 % MWCNT (see on the right).

All samples show high values in the storage modulus in the usual operational temperature range of structural materials. The profile of the curves in Fig. 2 shows a slow and progressive decrease of E' up to 50°C, followed by an almost constant value in the range between 50 ÷ 200 °C before the principal drop, due to

the glass transition temperature Tg which is evident between 200 ÷ 300 °C. The presence of the Tg in this range is also confirmed by the mechanical spectrum of the samples shown in Fig. 3.

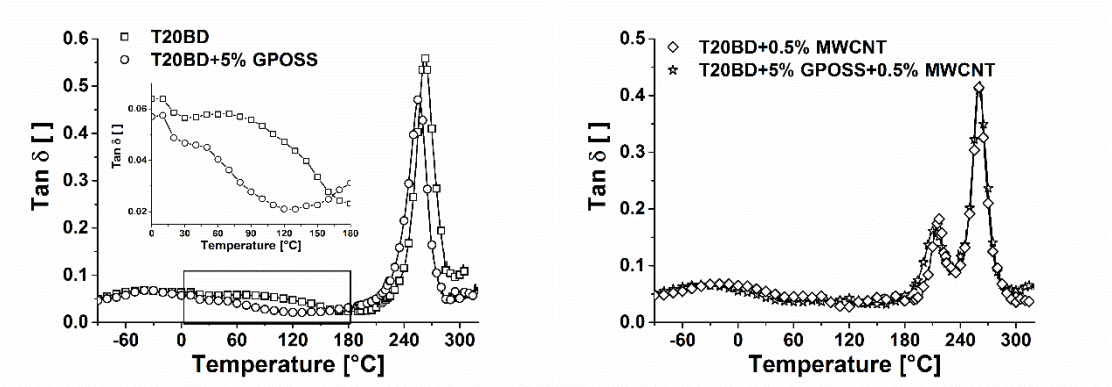

Fig. 3. Loss factor (tanδ) of the unfilled epoxy formulations T20BD, T20BD+5%GPOSS (see on the left); Loss factor (tanδ) of the epoxy formulations loaded with 0.5% by wt of MWCNT: T20BD+0.5% MWCNT, T20BD+5%GPOSS+0.5 % MWCNT (see on the right).

The formulation T20BD+5%GPOSS+0.5%MWCNT is characterized by a different profile of the curve related to the loss factor. In particular, a lower transition in the mechanical spectra at about 217°C is observed indicating the presence of a phase with greater mobility of chain segments. MWCNT are responsible for forming in the resin a second phase characterized by different crosslinking density. In this regard, it can be noticed that a single Tg at the temperature of about 260°C is observed for the unfilled samples T20BD and T20BD+5%GPOSS. The inset in Fig. 3 related to the loss factor of the unfilled epoxy formulations T20BD and T20BD+5%GPOSS highlights that the presence of the liquid GPOSS inside the epoxy matrix reduces the intensity of the γ transition (between 30 and 120÷140°C). The lower intensity of the γ transition for the sample T20BD+5%GPOSS may be due to a reduction of the material inhomogeneity related to regions of different crosslink density.

In order to better understand the influence of GPOSS and MWCNT on the dynamic mechanical properties of the samples, the storage modulus and the loss factor (tanδ) of the unfilled T20BD and T20BD+5% GPOSS+0.5 % MWCNT epoxy formulations are shown in Fig. 4.

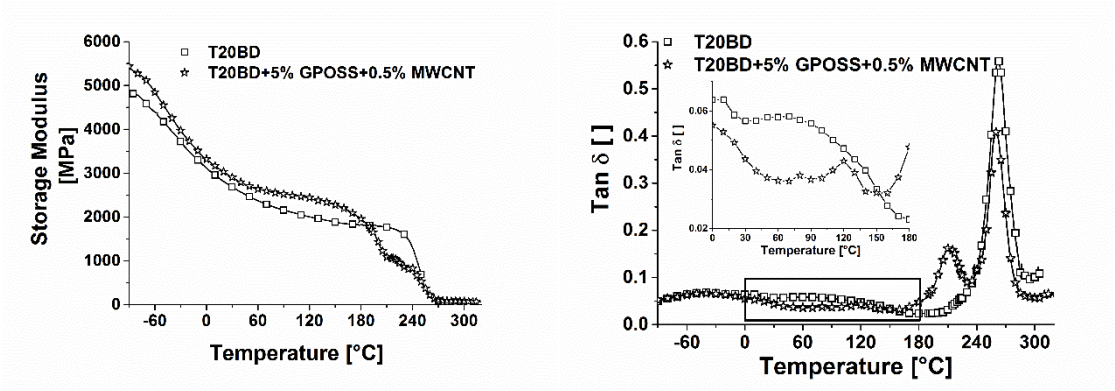

Fig. 4. Storage Modulus of the unfilled T20BD and T20BD+5%GPOSS+0.5%MWCNT epoxy formulations (see on the left); Loss factor (tanδ) of the unfilled T20BD and T20BD+5%GPOSS+0.5%MWCNT epoxy formulations.

A comparison between the storage modulus of the analyzed samples (Figs. 2 and 4 on the left) evidences that the presence of GPOSS has no influence on the values of storage modulus in the analyzed temperature range, whereas the carbon nanotubes determine a reinforcing effect, which does not seems to be related to the presence of GPOSS. Similarly, a comparison between the loss factor (tanδ) of the analyzed samples (Figs. 3 and 4 on the right) highlights that GPOSS nanocages are no responsible for the transition at lower temperature in the profile of the curve related to the loss factor.

3.2. Evaluation of the self-healing activity in the solid epoxy samples

The healing efficiency can be evaluated from the evolution of the relative elastic modulus during time. The dynamic test defines mechanical behavior responding to a continuously deformation, and it can be used to identify the recovery time and the amount mechanical healing. In this particular case, the relative elastic modulus G_r is defined as:

$$G_r = \frac{G - G_c}{G_p - G_c}$$

where G is the actual elastic modulus, G_c is the elastic modulus found just after the crack formation and G_p is the elastic modulus of the sample before the crack formation. Fig. 5 shows the time evolution curves of the relative elastic modulus of the formulations T20BD+5%GPOSS+0.5%MWCNT, T20BD+0.5%MWCNT and T20BD+5%GPOSS.

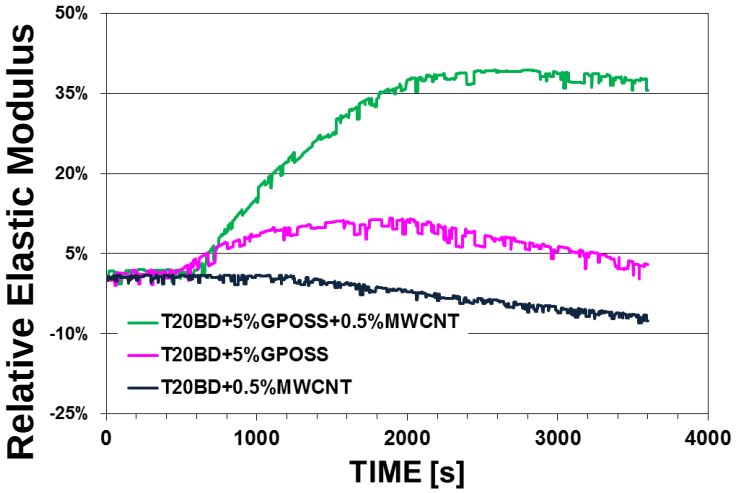

Fig. 5. Time evolution of the relative elastic modulus of the formulations T20BD+5%GPOSS+0.5%MWCNT, T20BD+0.5%MWCNT and T20BD+5%GPOSS.

Data in Fig. 5 highlight that the relative elastic modulus evolution of the samples showing self-healing ability (T20BD+5%GPOSS+0.5%MWCNT, T20BD+5%GPOSS) is quite similar for both samples. In particular, the samples show a maximum in the healing, followed by a slight drop probably due to the crack propagation caused by the cyclic fatigue stress. On the contrary, the healing efficiency, defined as the percentage of elastic modulus recovered, was found very different for the two samples (~40% for sample T20BD+5%GPOSS+0.5%MWCNT and ~10% for sample T20BD+5%GPOSS). No healing efficiency was found in the reference sample T20BD+0.5%MWCNT, highlighting how MWCNT do not impart self-healing functionality to the epoxy mixture. A complete list of the results obtained on the compositions analyzed in this work is shown in Table 1.

Table 1. Self-healing efficiency values of the different compositions analyzed.

Nr.	Samples	Self-healing efficiency (%)
1	T20BD+5%GPOSS+0.5%MWCNT	40±5
2	T20BD+5%DPHPOSS+0.5%MWCNT	45±5
3	T20BD+5%ECPOSS+0.5%MWCNT	30±5
4	T20BD+5%GPOSS	10±5
5	T20BD+5%DPHPOSS	15±5
6	T20BD+5%ECPOSS	15±5
7	T20BD+5%TCPOSS	20±5

Results clearly show that:

a) POSS compounds are able to impart self-healing efficiency to the resin formulation (see samples 4-7);

b) MWCNTs embedded in the epoxy formulation are able to increase the self-healing efficiency of about 400% (see sample 1).

The very interesting result of this investigation is the synergic effect between MWCNT and GPOSS for the activation of reversible hydrogen bonds inside the resin. Considering the structure and composition of GPOSS (see Fig. 6). A self-healing ability based on the presence of oxygen atoms which are able to form attractive reversible interactions (hydrogen bonding) with hydrogen covalently bonded to other oxygen atoms of the resin is expected (Fig. 7).

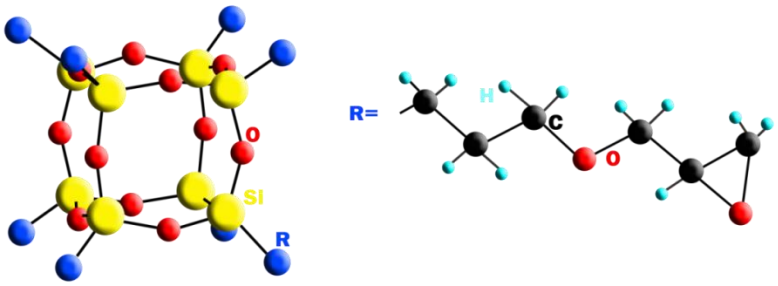

Fig. 6. Molecular/Chemical Formula of GPOSS, $(C_6H_{11}O_2)_n(SiO_{1.5})_n$ n=8,10,12 Molecular Weight: 1337.88 (for n = 8).

Samples with GPOSS which have manifested the highest increase in the self-healing efficiency have been chosen to understand why the presence of carbon nanotubes significantly increases the self-healing efficiency and therefore the ability to form reversible hydrogen bond.

It is worth noting that the result concerning the samples 1-2 of Table 1 are very promising. Even if the self-healing efficiency is between 40% – 45 % (hence lower than the healing efficiency of the microencapsulated systems [19, 21-23]), this samples are obtained from an epoxy mixture solidified with primary aromatic amines and therefore characterized by high values in the glass transition temperature and storage modulus as shown in the next section. This formulation is also characterized by improved flame resistance and electrical conductivity [45-46].

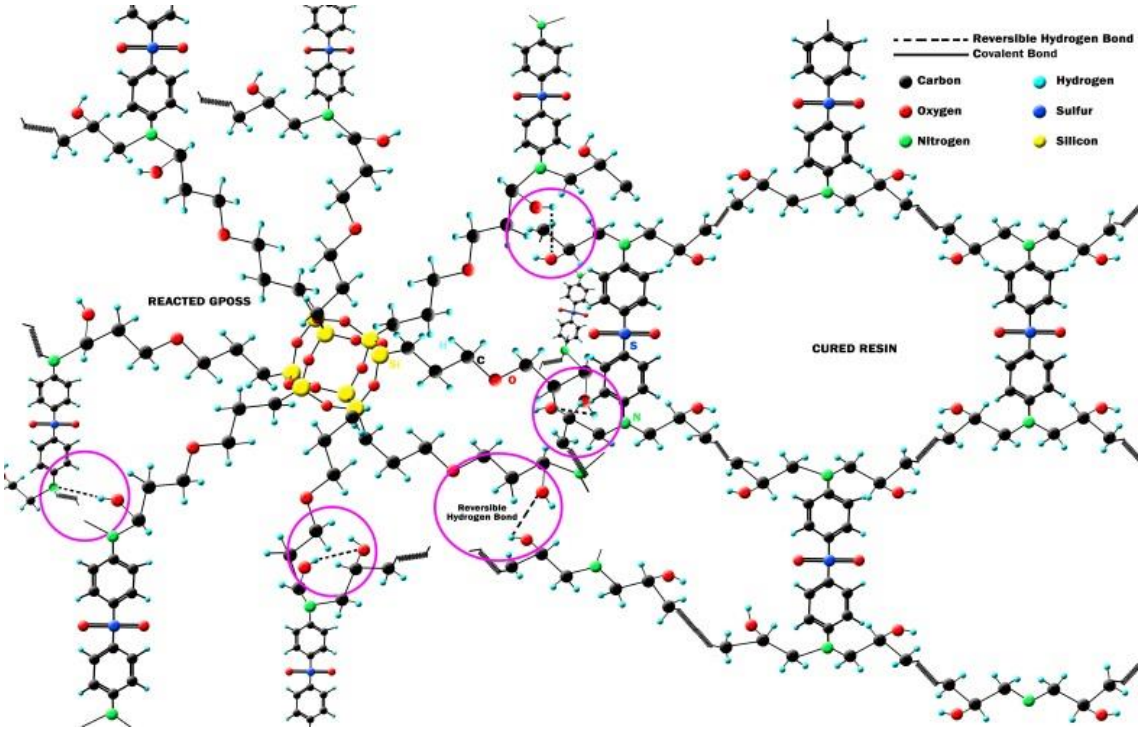

Fig. 7. Scheme of self-healing mechanisms based on reversible hydrogen bonds.

As discussed before, the healing efficiency has increased up to 400% for the resin containing GPOSS filled with MWCNT. It is therefore possible, and indeed likely, that the enhancement in the self-healing efficiency is due to the presence of this more mobile phase where the arrangements to create reversible hydrogen bonds (as illustrated in scheme of Fig. 7) are favored because of the increased mobility of the segment chains. Such a mechanism might also explain other data already reported in the literature for this system.

The results related to the crack growth rate measurement on double cantilever beam (DCB) specimens made of a Carbon Fiber Reinforced Composites (CFRCs) impregnated with the multifunctional epoxy composite T20BD+5% GPOSS+0.5 % MWCNT are characterized by a decrease in the fatigue crack growth rate by approximately 80%. This decrease could be due to the strengthening of hydrogen bonds, which are able to give strong cumulative effects able to modify delamination properties of the CFRCs [47].

3.3. Rheological Investigation

Formulation T20BD with GPOSS is characterized by reduced viscosities compared to the pristine epoxy formulation and that containing only MWCNT. It also allows a decreasing of the viscosity of the epoxy mixture. Rheological tests were performed on the formulation T20BD+5% GPOSS+0.5 % MWCNT. In .

Table 2, viscosity values of nanofilled epoxy formulation are compared with viscosity values of pristine epoxy mixture, and epoxy mixture with 0.5% of MWCNT, demonstrating the beneficial effect of GPOSS in lowering viscosity of system.

Table 2. Values of the viscosity η* [Pa s] at different temperatures for pristine resin and filled formulations.

Temperature [°C]	η* [Pa s] T20BD 5%GPOSS+ 0.5%MWCNT	η* [Pa s] T20BD	η* [Pa s] T20BD+0.5% MWCNT
80	2.33	5.26	7.83
90	1.43	2.11	5.82
100	0.94	0.96	4.49
110	0.77	0.52	3.58
120	0.68	0.31	3.05

3.4. Morphological Investigation

The MWCNT dispersion in the polymeric matrix both in presence and absence of GPOSS was analysed by SEM investigation on etched samples. The etching procedure consumes part of the surface layers of the epoxy matrix making possible a clearer observation of the dispersion state of the nanofiller, as already experienced with resins filled with carbon based nanofiller [26-27].

Fig. 8 shows SEM images at different magnifications of the fracture surface of the two epoxy-based composites filled at loading rate of 0.5 wt% of MWCNTs with GPOSS and in absence of GPOSS. The observation of the image in Fig. 8 highlights that, in both cases, the nanofillers seem uniformly dispersed in the polymeric matrix, but in the case of the matrix containing GPOSS, the nanotubes seem better dispersed in the resin. This better distribution could be due to the decrease in the viscosity of the matrix containing GPOSS which also allows a better nanofiller dispersion making the phase at higher mobility (see transition at lower temperature in the loss factor curve of the sample T20BD+5%GPOSS+0.5% MWCNT) well dispersed in the composite.

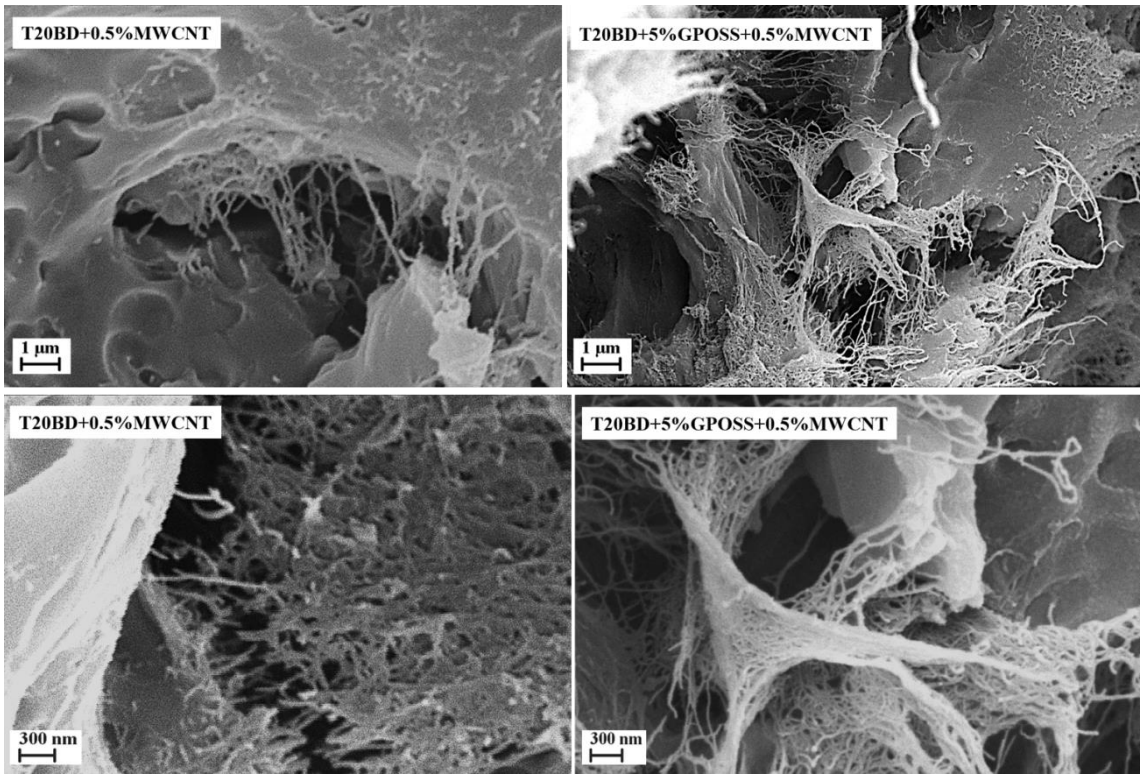

Fig. 8. SEM images at different magnifications of the fracture surface of the two epoxy-based composites filled with 0.5 wt% loading of MWCNTs with GPOSS and in absence of GPOSS.

3.5. Spectroscopic analysis

Infrared spectroscopy can be used to observe the O-H stretching band in the region between 3200 – 3650 cm^{-1}. This vibration is sensitive to hydrogen bonding. Generally, sharp bands related to this vibration are never observed in the FT/IR spectra of epoxy resins because they are related to free hydroxyl groups which can be observed in the vapor phase, in very dilute solution of non-polar solvents or for hindered OH groups. In these last cases, the additional formation of intermolecular hydrogen bonding appears as additional bands at lower frequencies between 3550-3200 cm^{-1}. In the solid state, the O-H stretching signal of an epoxy resin appears as a broad band because of the intermolecular hydrogen bonding formed during the curing cycle [48]. However, the profile of the band in the region of the hydroxyl groups and the presence of more or less accentuated shoulders and/or additional peaks can provide information about the nature of hydrogen bonding interactions. Fig. 9 shows the FT/IR spectra of the samples T20BD, T20BD+5%GPOSS and T20BD+5%GPOSS+0.5%MWCNT. Although the maximum intensity of the signal is almost the same for the three samples (~ 3399 cm^{-1}), the comparison of the spectra highlights different profiles of the O-H stretching band.

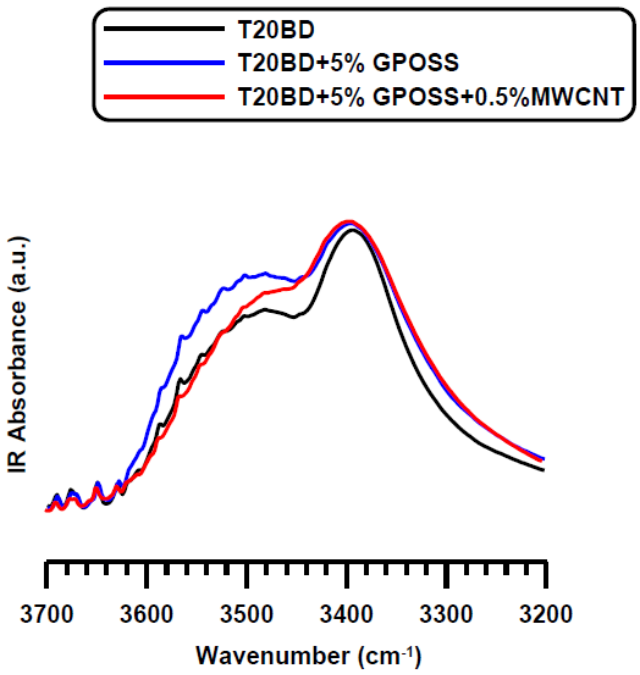

Fig. 9. FT/IR spectra of the samples T20BD, T20BD+5%GPOSS and T20BD+5%GPOSS+0.5%MWCNT.

For the sample T20BD+5%GPOSS+0.5%MWCNT (red spectrum), the presence of a less pronounced peak at higher frequency (~3482 cm^{-1}) and the widening of the band at lower frequencies (on the right side) is a clear indication of additional hydrogen bonding interactions with respect to those of sample T20BD. A comparison between the two samples containing GPOSS (blue and red spectra) also evidences that the inclusion of MWCNT seems to reduce the signal at higher frequency (3482 cm^{-1}) thus favoring intermolecular hydrogen bonding at the expense of the more "free" hydroxyl signals. It is very likely that the phase at higher mobility, due to interactions between CNTs and epoxy resin, facilitates molecular configurations allowing hydrogen bonding interactions.

4. Conclusions

The presence of GPOSS in the nanofilled epoxy matrix allows a decrease in the resin viscosity. This is a desirable effect as it count-balances the increase of the viscosity due to the addition of nanofillers in the epoxy. formulation. This increase in viscosity causes several processing problems such as difficulties in the dispersion stage of the nanofiller and/or filtration during the infusion process for the manufacture of carbon fiber reinforced composites. Dynamic mechanical results have shown that sample containing MWCNT tend to create a phase with increased mobility of the chains. This particular phase arrangement is most likely responsible to better promote reversible hydrogen bonds determined by interaction between epoxy resin

and nanocages of POSS compounds. The presence of a more mobile phase in the multifunctional formulation can be advantageously exploited to enhance the self-healing efficiency up to 400% and then to strongly reduce the fatigue crack growth rate of CFRs laminates impregnated with multifunctional formulations.

Acknowledgements

The research leading to these results has received funding from the European Union's Seventh Framework Programme for research, technological development and demonstration under Grant Agreement N° 313978.

References

1. White SR, Sottos NR, Geubelle PH, Moore JS, Kessler MR, Sriram SR, et al. Autonomic healing of polymer composites. Nature 2001;409:794-7.
DOI:10.1038/35057232

2. (a) Moll JL, White SR, Sottos NR. A Self-sealing Fiber-reinforced Composite. J Compos Mater 2010; 44(22):2573-85. DOI:10.1177/002199830935660 (b) Wilson GO, Moore JS, White SR, Sottos NR, Andersson HM. Autonomic Healing of Epoxy Vinyl Esters via Ring Opening Metathesis Polymerization. Adv Funct Mater 2008;18(1):44-52. DOI:10.1002/adfm.200700419 (c) Brown EN,White SR, Sottos NR. Retardation and repair of fatigue cracks in a microcapsule toughened epoxy composite-Part II: In situ self-healing. Compos Sci Technol 2005;65(15-16):2474-80. DOI:10.1016/j.compscitech.2005.04.053

3.(a) Schunack M, Gragert M, Döhler D, Michael P, Binder WH. Low-Temperature Cu(I)-Catalyzed "Click" Reactions for Self-Healing Polymers. Macromol Chem Phys 2012;213(2):205-14. DOI:10.1002/macp.20110037 (b) Döhler D, Michael P, Binder WH. Autocatalysis in the Room Temperature Copper(I)-Catalyzed Alkyne–Azide "Click" Cycloaddition of Multivalent Poly(acrylate)s and Poly(isobutylene)s. Macromolecules 2012;45(8):3335-45. DOI:10.1021/ma300405v (c) Gragert M, Schunack M, Binder WH. Azide/Alkyne-"Click"-Reactions of Encapsulated Reagents: Toward Self-Healing Materials. Macromol Rapid Commun 2011;32(5):419-25. DOI:10.1002/marc.201000687

4. Billiet S, Van Camp W, Hillewaere XKD, Rahier H, Du Prez FE. Development of optimized autonomous self-healing systems for epoxy materials based on maleimide chemistry. Polymer 2012;53(12):2320-6. DOI:10.1016/j.polymer.2012.03.061

5. Brown EN, White SR, Sottos NR. Microcapsule induced toughening in a self-healing polymer composite. Journal of Materials Science 2004;39(5):1703-10. DOI:10.1023/B:JMSC.0000016173.73733.dc

6. Rule JD, Sottos NR, White SR, Moore JS. The chemistry of self-healing polymers. Education in Chemistry 2005;42(5):130-2.

7. Rule JD, Brown EN, Sottos NR, White SR, Moore JS. Wax-protected catalyst microspheres for efficient self-healing materials. Advanced Materials 2005;17(2):205-8. DOI:10.1002/adma.20040060

8. Jones AS, Rule JD, Moore JS, White SR, Sottos NR. Catalyst morphology and dissolution kinetics of self-healing polymers. Chemistry of Materials 2006;18(5):1312-7. DOI:10.1021/cm051864s

9. Kessler MR, White SR. Self-activated healing of delamination damage in woven composites. Composites Part A: Applied Science and Manufacturing 2001;32(5):683-99. DOI:10.1016/S1359-835X(00)00149-4

10. Kessler MR, Sottos NR,White SR. Self-healing structural composite material. Composites Part A: Applied Science and Manufacturing 2003;34(8):743-53. DOI:10.1016/S1359-835X(03)00138-6

11. Brown EN, White SR, Sottos NR. Retardation and repair of fatigue cracks in a microcapsule toughened epoxy composite - Part I: Manual infiltration. Composites Science and Technology 2005;65:2466-73. DOI:10.1016/j.compscitech.2005.04.020

12. Jones AS, Rule JD, Moore JS, Sottos NR,White SR. Life extension of self-healing polymers with rapidly growing fatigue cracks. Journal of the Royal Society Interface 2007;4(13):395-403. DOI:10.1098/rsif.2006.0199

13. Toohey KS, Sottos NR, Lewis JA, Moore JS, White SR.Self-healing materials with microvascular networks. Nature Materials 2007;6(8):581-5. DOI:10.1038/nmat1934

14. Van der Zwaag S 2007 Self Healing Materials: An Alternative Approach to 20 Centuries of Materials Science (Springer Series in Materials vol 100) (Berlin: Springer)

15. Dry C 2007 Multiple function, self-repairing composites with special adhesives Int Patent WO/2007/005657

16. Motuku M, Vaidya UK, Janowski GM. Parametric studies on self-repairing approaches for resin infused composites subjected to low velocity impact. Smart Materials and Structures 1999;8(5):623-38. DOI:10.1088/0964-1726/8/5/313

17. Brown EN, Kessler MR, Sottos NR,White SR. In situ poly(urea-formaldehyde) microencapsulation of dicyclopentadiene. J. Microencapsulation 2003;20(6):719-30. DOI:10.1080/0265204031000154160

18.Guadagno L, Longo P, Raimondo M, Naddeo C, Mariconda A, Vittoria V, et al. Use of Hoveyda-Grubbs' second generation catalyst in self-healing epoxy mixtures. Composites Part: B Engineering 2011;42(2):296-301. DOI:10.1016/j.compositesb.2010.10.011

19. Guadagno L, Raimondo M, Naddeo C, Longo P, Mariconda A, Binder WH. Healing efficiency and dynamic mechanical properties of self-healing epoxy systems. Smart Materials and Structures 2014;23(4):045001 (11 pp). DOI:10.1088/0964-1726/23/4/045001

20. Wilson GO, Caruso MM, Reimer NT, White SR, Sottos NR, More JS. Evaluation of ruthenium catalysts for ring-opening metathesis polymerization-based self-healing applications. Chem Mater 2008;20(10):3288-97 (Supporting Information). DOI:10.1021/cm702933h

21. Raimondo M, Longo P, Mariconda A, Guadagno L. Healing agent for the activation of self-healing function at low temperature. Adv Compos Mater 2015;24(6):519-29. DOI:10.1080/09243046.2014.937135

22. Raimondo M, Guadagno L. Healing efficiency of epoxy-based materials for structural applications. Polymer Composites 2013;34(9):1525-32. DOI:10.1002/pc.22539

23. Guadagno L, Raimondo M, Naddeo C, Longo P, Mariconda A. Self-healing materials for structural applications. Polymer Engineering & Science 2014;54(4):777-84. DOI:10.1002/pen.23621

24. Guadagno L, Mariconda A, Agovino A, Raimondo M, Longo P. Protection of graphene supported ROMP catalyst through polymeric globular shell in self-healing materials. Composites Part B: Engineering 2017;116:352-60. DOI: 10.1016/j.compositesb.2016.10.075

25. Mariconda A, Longo P, Agovino A, Guadagno L, Sorrentino A, Raimondo M. Synthesis of ruthenium catalysts functionalized graphene oxide for self-healing applications. Polymer 2015;69:330-42. DOI:10.1016/j.polymer.2015.04.048

26. Guadagno L, Naddeo C, Raimondo M, Barra G, Vertuccio L, Russo S, et al. Influence of carbon nanoparticles/epoxy matrix interaction on mechanical, electrical and transport properties of structural advanced materials. Nanotechnology 2017;28(9):094001. DOI:10.1088/1361-6528/aa583d

27. Guadagno L, Raimondo M, Vertuccio L, Mauro M, Guerra G, Lafdi K, et al. Optimization of graphene-based materials outperforming host epoxy matrices. RSC Adv 2015;5(46):36969-78. DOI:10.1039/C5RA04558D

28. Glaskova-Kuzmina T, Aniskevich A, Zarrelli M, Martone A, Giordano M. Effect of filler on the creep characteristics of epoxy and epoxy-based CFRPs containing multi-walled carbon nanotubes. Composites Science and Technology 2014;100:198-203. DOI: 10.1016/j.compscitech.2014.06.011

29. Zotti A, Borriello A, Martone A, Antonucci V, Giordano M, Zarrelli M. Effect of sepiolite filler on mechanical behaviour of a bisphenol A-based epoxy system. Composites Part B: Engineering 2014;67:400-9. DOI: 10.1016/j.compositesb.2014.07.017

30. Zotti A, Borriello A, Ricciardi M, Antonucci V, Giordano M, Zarrelli M. Effects of sepiolite clay on degradation and fire behaviour of a bisphenol A-based epoxy. Composites Part B: Engineering 2015;73:139-48. DOI: 10.1016/j.compositesb.2014.12.019

31. Vietri U, Guadagno L, Raimondo M, Vertuccio L, Lafdi K. Nanofilled epoxy adhesive for structural aeronautic materials. Composites Part B: Engineering 2014;61:73-83. DOI: 10.1016/j.compositesb.2014.01.032

32. Vertuccio L, Guadagno L, Spinelli G, Lamberti P, Tucci V, Russo S. Piezoresistive properties of resin reinforced with carbon nanotubes for health-monitoring of aircraft primary structures. Composites Part B: Engineering 2016;107:192-202. DOI: 10.1016/j.compositesb.2016.09.061

33. Ma HL, Jia Z, Lau KT, Lid X, Hui D, Shi SQ. Enhancement on mechanical strength of adhesively-bonded composite lap joints at cryogenic environment using coiled carbon nanotubes. Composites Part B: Engineering 2017;110:396-401. DOI: 10.1016/j.compositesb.2016.11.019

34. Zakaria MR, Abdul Kudus MH, Md. Akil H, Mohd Thirmizir MZ. Comparative study of graphene nanoparticle and multiwall carbon nanotube filled epoxy nanocomposites based on mechanical, thermal and dielectric properties. Composites Part B: Engineering 2017;119:57-66. DOI: 10.1016/j.compositesb.2017.03.023

35. Gaztelumendi I, Chapartegui M, Seddon R, Flórez S, Pons F, Cinquin J. Enhancement of electrical conductivity of composite structures by integration of carbon nanotubes via bulk resin and/or buckypaper films. Composites Part B: Engineering 2017;122:31-40. DOI: 10.1016/j.compositesb.2016.12.059

36. Kwon YJ, Kim Y, Jeon H, Cho S, Lee W, Lee JU. Graphene/carbon nanotube hybrid as a multi-functional interfacial reinforcement for carbon fiber-reinforced composites. Composites Part B: Engineering 2017;122:23-30. DOI: 10.1016/j.compositesb.2017.04.005

37. Viscardi M, Arena M, Barra G, Guadagno L. Structural performance analysis of smart carbon fiber samples supported by experimental investigation. International Journal of Mechanics 2016;10:376-82.

38. Martone A, Antonucci V, Zarrelli M, Giordano M. A simplified approach to model damping behaviour of interleaved carbon fibre laminates. Composites Part B: Engineering 2016;97:103-10. DOI: 10.1016/j.compositesb.2016.04.048

39. Nicole L, Rozes L, Sanchez C. Integrative approaches to hybrid multifunctional materials: from multidisciplinary research to applied technologies. Advanced Materials 2010;22(29):3208-14. DOI:10.1002/adma.201000231

40. Potier F, Guinault A, Delalande S, Sanchez C, Ribot F, Rozes L. Nano-building block based-hybrid organic–inorganic copolymers with self-healing properties. Polym Chem 2014;5(15):4474-9. DOI:10.1039/C4PY00172A

41. Guadagno L, Raimondo M, Vietri U, Vertuccio L, Barra G, De Vivo B, et al. Effective formulation and processing of nanofilled carbon fiber reinforced composites. RSC Adv 2015;5(8):6033-42. DOI:10.1039/C4RA12156B

42. Guadagno L, Vietri U, Raimondo M, Vertuccio L, Barra G, De Vivo B, et al. Correlation between electrical conductivity and manufacturing processes of nanofilled carbon fiber reinforced composites. Composites Part B: Engineering 2015;80:7-14. DOI: 10.1016/j.compositesb.2015.05.025

43. Martone A, Formicola C, Piscitelli F, Lavorgna M, Zarrelli M, Antonucci V, et al. Thermo-mechanical characterization of epoxy nanocomposites with different carbon nanotube distributions obtained by solvent aided and direct mixing. eXPRESS Polymer Letters 2012;6(7):520-31. DOI: 10.3144/expresspolymlett.2012.5

44. Guadagno L, Raimondo M, Vittoria V, Vertuccio L, Naddeo C, Russo S, et al. Development of epoxy mixtures for application in aeronautics and aerospace. RSC Adv 2014;4(30):15474-88. DOI:10.1039/C3RA48031C

45. Raimondo M, Russo S, Guadagno L, Longo P, Chirico S, Mariconda A, et al. Effect of incorporation of POSS compounds and phosphorous hardeners on thermal and fire resistance of nanofilled aeronautic resins. RSC Adv 2015;5(15):10974-86. DOI:10.1039/C4RA11537F

46. Guadagno L, Raimondo M, Longo P, Bonnaud L, Murariu O, Dubois Ph, Russo S, Iannuzzo G. Multifunctional epoxy resin with enhanced flame resistance, 2015, EUROPEAN PATENT APPLICATION EP2883896 (A1), Also published as: ITTO20131021 (A1) - Resina epossidica multifunzionale con accresciuta resistenza alla fiamma.

47. Kadlec M, Nováková L, Mlch I, Guadagno L. Fatigue delamination of a carbon fabric/epoxy laminate with carbon nanotubes. Compos Sci Technol 2016;131:32-39. DOI: 10.1016/j.compscitech.2016.05.013

48. Guadagno L, Raimondo M, Naddeo C, Russo S, Vittoria V, Russo S, Iannuzzo G. Dynamic Mechanical Properties of Structural Self-Healing Epoxy Resins. Applied Mechanics and Materials 2011;62:95-105. DOI: 10.4028/www.scientific.net/AMM.62.95